Cell Reports, Volume *19*

Supplemental Information

Huntington's Disease iPSC-Derived Brain Microvascular Endothelial Cells Reveal WNT-Mediated Angiogenic and Blood-Brain Barrier Deficits

Ryan G. Lim, Chris Quan, Andrea M. Reyes-Ortiz, Sarah E. Lutz, Amanda J. Kedaigle, Theresa A. Gipson, Jie Wu, Gad D. Vatine, Jennifer Stocksdale, Malcolm S. Casale, Clive N. Svendsen, Ernest Fraenkel, David E. Housman, Dritan Agalliu, and Leslie M. Thompson

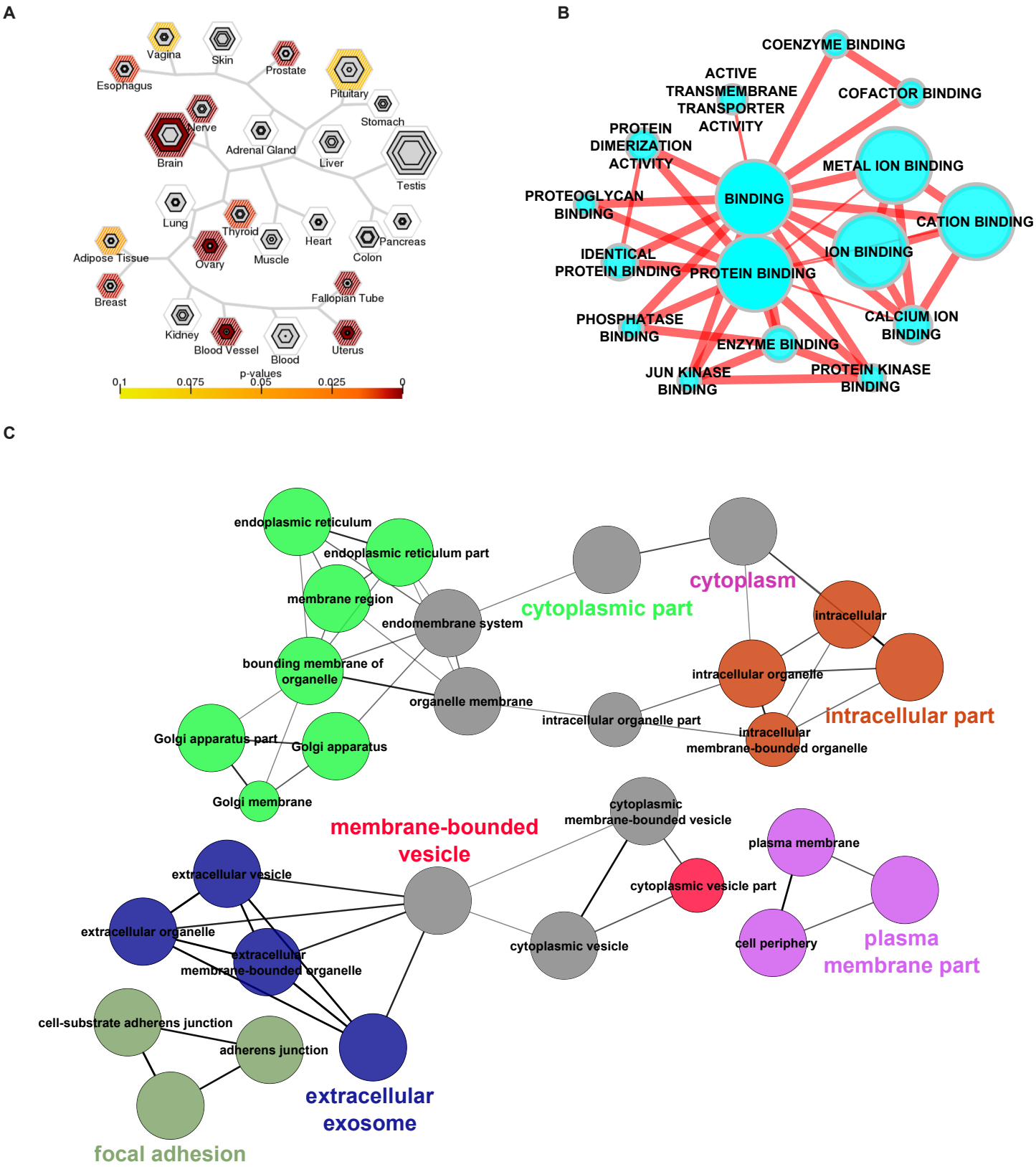

Figure S1. Cytoscape networks displaying GO functional analysis. Related to Figure 5. A) Enrichment mapping of binGO molecular functional analysis shows enrichment of genes that control ion binding, including INTEGRINS. B) CluGO analysis showing enrichment of specific cellular compartments. Analysis revealed enrichment of cytoplasmic and plasma membrane localized genes and lack of enrichment for nuclear genes. A & B) All enrichment nodes have an adjusted p-value < 0.05. Adjusted p-values were calculated based on overrepresentation of categories over a background sample using a hypergeometric test and adjusted using a Benjamini & Hochberg FDR.

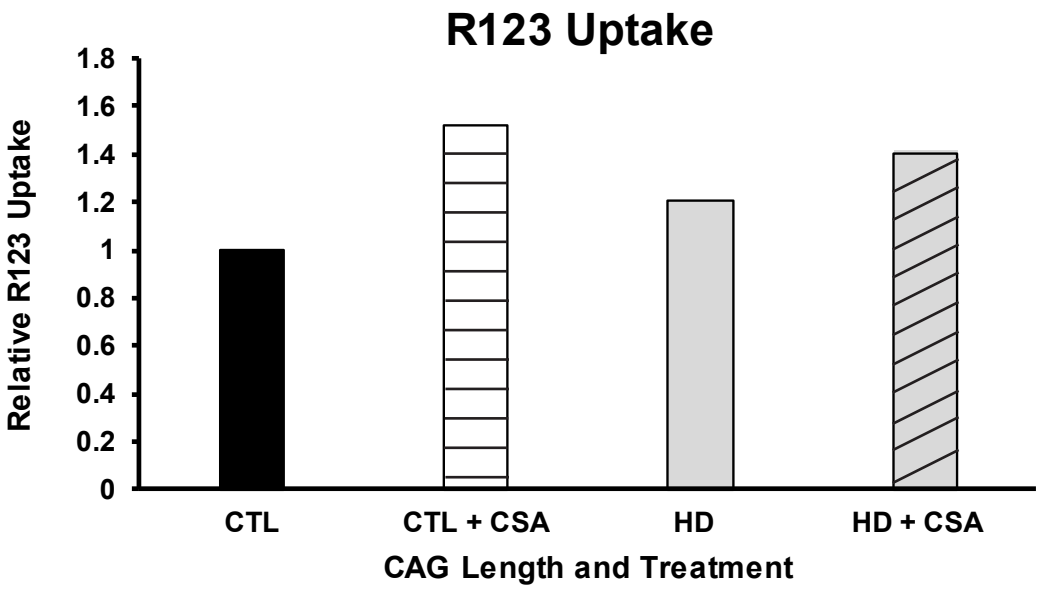

Figure S2. MDR1 function is inhibited in iBMECs by cyclosporine A treatment. Related to Figure 3. Flow cytometry quantification of Rhodamine 123 efflux/uptake in control (28Q + 33Q) and HD (66Q) iBMECs treated with vehicle or cyclosporine A (CSA).

Cell line	Clone	Gender	Diagnosis	CAG repeats	Coriell Catalog ID (fibroblasts)	Reference
CS14iCTR28 (28Q)	n6	FEMALE	Clinically normal	28	GM03814	Sareen et al. (2013)
CS83iCTR33 (33Q)	n1	FEMALE	Clinically normal	33	GM02183	Sareen et al. (2013)
CS21iHD60 (60Q)	n8	FEMALE	HD	60	GM03621	Mattis et al. (2015)
CS02iHD44 (66Q)	n4	FEMALE	HD	66	Submitted, pending - HDF2 Q66	N/A
CS81iHD71 (71Q)	n3	FEMALE	HD	71	GM04281	N/A
CS09iHD109 (109Q)	n1	FEMALE	HD	109	2024-7206 HD-109 Q	Mattis et al. (2015)

Table S1. Data on Cell lines used in studies. Relate to Figure 1.

Cell line	HTT expression (mean FPKM)	Ethnicity	Age	Age of onset	Additional Clinical Characteristics
CS14iCTR28 (28Q)	5.720468	Caucasian	Unknown	N/A	Clinically unaffected mother of two affected children: (1st child is GM03813/GM23240/GM24468 and 2nd child is not in repository); PCR analysis reveals donor subject has 3 or more copies of the SMN2 gene (data from several sources including Stabley et al. 2015, PMID 26247043) and is heterozygous for deletion of exons 7 and 8 in the SMN1 gene; unstable cytogentically; see GM24474 (iPSC-episomal) and ND41114/ND42240/ND42240 (iPSC clones-episomal). Chromosomal Location: 5q12.2-q13.3
CS83iCTR33 (33Q)	6.096943	Caucasian	21 YR (At Sampling)	N/A	At risk (50%)
CS21iHD60 (60Q)	4.711555	Caucasian	29 (At sampling)	18	onset at age 18 years; HTT CAG repeats are 18 and 60; similarly affected grandmother and father
CS02iHD44 (66Q)	4.783843	Caucasian	20 (At sampling)	~16	Onset at approximately 16 years. HTT CAG repeats are 21 and 66. Family history unknown.

CS81iHD71 (71Q)	**5.025625**	**Caucasian**	**20 YR (At Sampling)**	**14**	**Code 48; rigid form of HD; possible homozygote; both parents affected; onset at age 14 years; neurological exam 3/82 shows a hypokinetic variant of HD with dystonia and marked tremor, ataxic wide-based gait**
CS09iHD109 (109Q)	**4.84312**	**Caucasian**	**9 YR (At Sampling**	**3**	**Juvenile onset form with severe bradykinesia, rigidity and dystonia at time of biopsy**

Table S2. Additional data on Cell lines used in studies. Relate to Figure 1 and Table S1.

Study	Cell Type	Isolation method	Purpose
Dieterich et al., 2012	Primary Human	LCM	Transcriptional Profiling of primary hBECs associated with glioblastoma
Giger, T. et al., 2010	Primary Human	LCM	Identify Genes preferentially expressed in endothelial cells
Geier, EG et al., 2013	Primary Human	Purification	Transcriptional Profiling of primary BMVs for SLC and ABC genes
Barbier et al., 2011	HBEC-5i	Culture	Transcription profiling of hBECs treated with TNF and co-cultured with platelets, +/- P.falciparum
Lopez-Ramirez et al., 2013	hCMEC/D3	Culture	identify the major molecular process involved in cytokine-induced changes in brain endothelial
Zhang et al., 2014	Primary Human	Purification	Transcriptional profiling of primary human brain cells including: BEC, neurons, and glia.

Table S3. Previous human BEC datasets used for comparison with the healthy control or HD patient iPSC-derived BMECs. Relate to Figure 1.

Gene Symbol
ABCA11P
ABCA2
ABCA7
ABCB4
ABCC6
ABCD4
SLC10A4
SLC10A7
SLC12A8
SLC13A3
SLC13A4
SLC15A2
SLC16A13
SLC16A1-AS1
SLC16A9
SLC18A2
SLC18B1
SLC1A6
SLC22A15
SLC22A17
SLC25A21-AS1
SLC25A38
SLC25A51
SLC26A11
SLC26A6
SLC27A2
SLC27A6
SLC29A4
SLC2A10
SLC2A11
SLC2A13
SLC2A14

SLC30A5
SLC30A6
SLC35C2
SLC35D1
SLC35E2
SLC35F6
SLC35G1
SLC38A10
SLC38A4
SLC38A7
SLC38A9
SLC39A4
SLC44A5

SLC45A4
SLC46A1
SLC4A3
SLC4A8
SLC52A2
SLC6A4
SLC6A9
SLC7A2
SLC7A5P1
SLC8B1
SLC9A3

Table S4. ABC-, SLC- and anti-sense SLC- genes that are uniquely expressed in iBMECs. Related to Figure 1.

motif_name	motif	pvalue
NRF-1	yGCGCakGCGC (959)	6.75E-12
GMEB2	t.ACGyam (1490)	7.32E-12
MIZF	c.rCGTCCGC (1352)	1.91E-08
Egr-1	mCgCCCACGC. (1128)	1.09E-07
HIC1	ss...TGCcc.... (1642)	2.70E-05
AhR, Arnt, HIF-1	rCGTG.g (1486)	2.73E-05
FPM315 (ZNF263)	s.gGGAGSAsg. (1563)	2.82E-05
HINFP1	GCGGACSyks.rSGTCCGC (487)	2.89E-05
ZIC1	grCCCCCyGCtG.G. (859)	4.67E-05
HINFP1	GCGGACGy.scrrCGTCCGC (466)	7.43E-05
AP-2	.gCCy..rGGca (1469)	0.00017329
Sp1	ggGGGcGGgg. (1671)	0.00017753
TFAP2A	tGCCc...gGGC. (1183)	0.00026828
DEAF1	c...yycggg.ryttCCG... (1220)	0.00054296
Elk-1	smGGAary. (1649)	0.00074553
HIF1	g...ACGTGc.g. (1199)	0.00106378
Egr	gyGGGsGsrrs (1524)	0.00221534
Whn	...gACGC.. (1313)	0.00287111
STAT3:STAT3	kTkmcGGGAAmtsc (597)	0.00766075
STAT1	......TTCCsGGAA.tg.s (619)	0.00962985
E2F	ttTsGCGSsm.. (957)	0.01416598
c-Myc:Max	.rcCACGTGgy. (796)	0.02019337
HSF	TTCcmGarGyTTC (529)	0.0257967

KLF15	grg..GGGG.Gkkg (1513)	0.02948602
ETS1	accGGAwryrcwTCCgs. (510)	0.03063619
AP-2	s...CC.c.GGC (1579)	0.03328093
Hmx3 (Nkx5-1)	CAAGTGCGTG (656)	0.03703764
CREB	y.aCGTCA. (1504)	0.0371707
Staf	.twCCCA.maTgCayyrcg.. (725)	0.03953917
CTF1	TTGGCa...tGCCAr (482)	0.04231066
MYBL1	g.csgTTa.wrCsGTtr (889)	0.04570253
GMEB2	yaCGtaac.saCGya (694)	0.04825038

Table S5. Motif analysis of SLC and ABC genes in iBMECs. Related to Figure 1. These sequence motifs are highly enriched when analyzing all SLC and ABC genes that are identified in our healthy control iBMECs. P-values represent the likelihood of finding the calculated enrichment of that motif in random sequences with similar GC content.

Table S6. Full differentially expressed gene list at 0.05 FDR. Related to Figure 4. Table is included as a separate Excel sheet.

motif_name	**Motif**	**p value**
SOX10	AACAATrTgCAGTGTT (184)	0.003848177
Whn	a..gACGC.. (2491)	0.007057183
XBP-1	.w..gmCACGtca. (2200)	0.021306218
MEF-2	rgyTaTwTTwA. (1197)	0.021878571
COUPTF	.....tGacCyyts..c.y..m (2680)	0.022486414
HIF1	g..kACGTGc.g. (2163)	0.026718534
SOX10	.AACAATTkCAGTGTT (306)	0.026993552
Pbx	.tCAATCw. (2257)	0.02772903
HINFP1	GCGGACsyks.rCGTCCGC (918)	0.033777487
HES5	yGgCACGTGCCr (1084)	0.046792929
BCL6	wrCTTTCkagGraT (969)	0.049745361
motif name	**Motif**	**p value**
Elk-1	acCGGAary (206)	0.00085818
E2F	tTTsGCGs (200)	0.035495641
CTCF	..gcCas.aGrkGGcrs (203)	0.045838048
Helios A	TTTCCw (291)	0.049393656

Table S7. Motif analysis of DEGs in HD iBMECs. Related to Figure 4. These sequence motifs are highly enriched near genes that are upregulated in HD-BMECs compared to control lines (top) or that are only expressed in HD-BMECs and not control lines (bottom). P-values represent the likelihood of finding the calculated enrichment of that motif in sequences upstream of genes that are downregulated in HD (top) or are only expressed in control lines (bottom).

Case #	Diagnosis	Age	Gender	Post-mortem interval	HD histopathological score
1	**Healthy control**	**79**	**F**	**8**	**N/A**
2	**Healthy control**	**62**	**M**	**6**	**N/A**
3	**Healthy control**	**54**	**F**	**22**	**N/A**
4	**Huntington's disease**	**75**	**F**	**38**	**2/4**
5	**Huntington's disease**	**72**	**M**	**31**	**2/4**
6	**Huntington's disease**	**50**	**F**	**37**	**2/4**

Table S8. Characteristics of human subjects used in this study. Related to Figure 5.

Target	Antibody	Dilution	Supplier
CD31	Rabbit	1:25	Thermo Scientific
GLUT-1	Mouse	1:200	Thermo Scientific
OCCLUDIN	Mouse	1:200(ICC)/ 1:500(WB)	Invitrogen
CLAUDIN-5	Mouse	1:250(ICC)/ 1:500(WB)	Invitrogen
ZO-1	Rabbit	1:250	Invitrogen
SOX-17	Mouse/Rabbit	1:25(IHC)/1:500(WB)	Acris/Abcam
CAV-1	Mouse	1:250	Invitrogen
PGP	Mouse	1:25	Thermo Fisher
ACTIN	Mouse	1:5000	Invitrogen

Table S9. Table of antibodies used in the study. Related to Experimental Procedures.

Table S10. Table of Statistical methodology. Related to Supplemental Experimental Procedures. Table showing number of *n*, statistical test and comparisons used for each experiment is included as a separate Excel sheet. The control cell line values were only used together for stat comparisons after ANOVA and posthoc showed no statistical difference between the two lines for each experiment.

Supplemental Experimental Procedures

Statistical Analysis. Multiple statistical models were used to test the data based on data parameters. For each experiment a description of the statistical model used can be found within the figure legend or methods. Statistical significance is denoted by * < 0.05, ** < 0.01, *** < 0.001. Sample sizes and statistical tests for each experiment were chosen based on previous expertise and knowledge from past experiments using similar model systems, mice and iPSCs, and current accepted standards based on literature review. An estimation of variation within control or HD samples was assessed based on the statistical model used or data acquired, and accounted for in each experiment. No significant differences were detected between control samples. Control values were then combined for further comparison to HD samples. Also see Table S10.

Generation and characterization of human non-integrating iPSCs using episomal plasmids

Fibroblasts were reprogrammed into non-integrating and virus-free iPSC lines as described (Mattis et al., 2015) using the Amaxa Human Dermal Fibroblast Nucleofector Kit to express episomal plasmids with six factors: OCT4, SOX2, KLF4, L-MYC, LIN28, and p53 shRNA (Addgene) (Mattis et al., 2015). Nomenclature reflects the 1) last two digits of parental lines identifier, 2) non-disease or HD line, 3) CAG repeat number, and 4) clone number (Mattis et al., 2015). Human iPSCs were rigorously characterized at the Cedars-Sinai iPSC core. G-Band karyotyping ensured normal a karyotype and genomic DNA PCR confirmed the absence of episomal plasmid genes, as described (Muller et al., 2011; Okita et al., 2011; Sareen et al., 2012). Pluripotency was assessed by immunostaining with surface and nuclear pluripotency markers for subsequent flow cytometry quantification (> 80% SSEA4 and Oct3/4 double positivity), by quantitative RT-PCR of endogenous pluripotency genes, and by gene-chip and bioinformatics-based PluriTest assays. Spontaneous embryoid body differentiation confirmed the capacity to form all germ layers. Additional HD lines (66Q, 71Q) were also generated and characterized using the same methods from either primary patient fibroblasts obtained from the University of California, Irvine under IRB protocol #2008-6556 (66Q) or from the Coriell NINDS Repository (71Q, GM04281) under approved consent and privacy guidelines (Mattis et al., 2015). CAG repeat lengths were determined following reprogramming and included in TableS1 & S2. All procedures were performed in accordance with the institutional review board's guidelines at the Cedars-Sinai Medical Center under the auspice IRB-SCRO Protocols Pro00028429 (Transplantation iPSC-derived human neural progenitors), Pro00021505, and Pro00032834.

Maintenance and differentiation of human iPSC-derived BMECs and iNPCs cells. Briefly, iPSCs underwent spontaneous differentiation for 6 days in unconditioned medium (UM). The mixed cultures were then switched to human endothelial cell medium (Life Technologies) with bFGF (R&D Systems) and 1% platelet-poor plasma derived bovine serum (Alfa Aesar) to select for BMEC colony expansion and maturation for 2 days. During this time the samples were treated with retinoic acid (RA, Sigma). All cells were then plated onto collagen-IV (Sigma) and fibronectin (Corning) coated tissue culture plates or 0.4 μM 12 well transwell filters for 2-3 days to reach confluence before characterization and use in various assays. For iNPCs cells EZ spheres were dissociated in Accutase and plated down on to matrigel coated plates or tranwell inserts.

Immunofluorescence & CLDN5 puncta.
After 2-3 days of growth on collagen IV and fibronectin coated chamber slides, cells were washed once with PBS and fixed in either 4% paraformaldehyde, 100% ice-cold methanol, or ice-cold 95% ethanol followed by 80% ice-cold acetone. Following fixation cells were blocked in 10% goat serum with 1% BSA and 0.1% triton X-100 (where applicable) for 1 hour at room temperature. Cells were then labeled with primary antibody overnight at 4 degrees, washed three times with PBS and treated with a fluorescently labeled secondary antibody for 1 hour at room temperature. Cells were counterstained with DAPI to visualize nuclei. Image J was used to quantify intracellular CLDN5 puncta using 3 images per a differentiation at 100x.

RNAseq and DE Statistics.
Total RNA was isolated from cells with the Qiagen RNeasy Kit using a QIAshredder for cell lysis and all RIN values were >9. RNA-Seq libraries were made with 1ug of RNA using the Illumina TruSeq mRNA v2 protocol. Libraries were quantified using the KAPA library quant kit and sequenced on the HiSeq 2500 using 75 cycles to obtain paired-end reads 75 base pairs in length. Paired-end reads were trimmed using a base quality score threshold of >20 and aligned to the hg19 genome with Tophat 2. RNA-Seq data were analyzed using quality control metrics, including: quality score trimming, base composition, k-mer content, and 5' and 3'- bias. Counts per gene were quantified using HTseq and analyzed with the R package DESeq2, or Partek Flow, to identify differentially expressed genes. 10% and 5% false discovery rate cutoffs were used for significance for DESeq2 and Partek Flow, respectively.

Exploratory, pathway, and motif analysis of DEGs.
For exploratory analysis plots GENE-E and Partek GS 6.6 were used for hierarchical clustering (Spearman's Ranked Correlation) and heatmap generation, and PCA of log2 transformed global expression values, respectively. Data were analyzed through the use of QIAGEN's Ingenuity® Pathway Analysis (IPA®, QIAGEN Redwood City, www.qiagen.com/ingenuity) for pathway analysis and upstream regulator analysis. Cytoscape was used to visualize GO analysis networks from BinGO, Enrichment Map, and CluGO (Bindea et al., 2009; Maere et al., 2005; Merico et al., 2010; Shannon et al., 2003). EnrichR was used for additional pathway analysis to obtain ChEA and ENCODE ChIPSeq enrichments (Chen et al., 2013; Kuleshov et al., 2016). Motif analysis was performed on a 1000bp region

upstream of each gene's TSS, as reported by RefSeq, which were taken from the hg19 genome. Background sequences were created by sampling the genome for the same number of random 1000bp regions of matched GC content (in the case of the healthy BMEC analysis) or by using the upstream regions from the opposite treatment group (when comparing HD patient-derived cells to healthy-patient derived cells). THEME (Macisaac et al., 2006) was used to find enriched motifs in the upstream regions over the background sequences. The set of motif hypotheses is derived from all vertebrate-specific scoring matrices (PSSMs) from TRANSFAC (Wingender et al., 1996) and the human HT-SELEX compendium (Jolma et al., 2013), filtered for sufficient information content (>9 total bits). Motif hypotheses were then clustered according to similar binding site motifs, and the top p-value for all motifs in a cluster is reported. Statistical analysis of SLC- and ABC genes were calculated using one-tailed p-value with a Chi squared test with Yates' correction.

Efflux and transporter Assays. For uptake assays cells were allowed to reach confluence on 6 well plate 2 days post subculture. The upper chamber medium was replaced with medium containing either 10 µM rhodamine 123 (Life Technologies) or 10 mM albumin-594 (Life Technogies) and incubated for 1 hour at 37 degrees C. After incubation cells were trypsinized, fixed with 4% PFA, and analyzed using flow cytometry for mean fluorescence. Gating were set using unstained and FMO controls. Puromycin efflux was measured based on cell death by allowing the BMECs to grow for 48 hours post subculture in normal 12 well TC plates with subsequent treatment with either 0.5 or 1 µM puromycin. After 48 hours of treatment cells were washed once with PBS and fixed with 4% PFA. After fixation cells were then washed and DAPI stained to visualize cell nuclei. ImageJ software was used to quantify cell counts from five images per a well using 3 wells per an experimental set and over 4 experiments.

Human Tissues. Western analysis primary antibodies were incubated in RIPA buffer containing protease inhibitors (HALT; Thermofisher), sonicated, concentrations determined by the Bradford method (Biorad), and suspended in Laemelli's sample buffer. 20ug protein per sample were electrophoresed on 4-15% acrylamide gels and probed with primary antibodies against human CLDN-5, OCCLUDIN, β-ACTIN (Invitrogen), SOX17 (Abcam). For IHC Deparaffinized sections underwent antigen retrieval for 35 min at 100°C (Target Retrieval Solution, pH 6; Dako, Carpinteria, CA). Peroxidase activity was quenched with 3% H_2O_2 for 10 min. Sections were blocked with 2.5% horse serum, incubated with SOX17 (Acris, Rockville, MD, Catalog # TA500281 at 1:25) for 18 h at 4°C, followed by ImmPRESS anti-mouse Ig peroxidase (Vector Labs, Burlingame, CA) and development with peroxidase-conjugated 3,3'-diaminobenzidine (Catalog # SK-4100; Vector Labs, Burlingame, CA). Washes were performed with 0.1% Tween-20 in PBS. Sections were counterstained with hematoxylin, then dehydrated and mounted with Permount. Images were captured using a Zeiss Axiomager microscope equipped with DIC optics using 20X objectives, Accumulation of DAB reaction product in endothelial nuclei was scored as 0=none detected, 1+=low, 2+=moderate, 3+=high.

Supplemental References

Bindea, G., Mlecnik, B., Hackl, H., Charoentong, P., Tosolini, M., Kirilovsky, A., Fridman, W.H., Pages, F., Trajanoski, Z., and Galon, J. (2009). ClueGO: a Cytoscape plug-in to decipher functionally grouped gene ontology and pathway annotation networks. Bioinformatics *25*, 1091-1093.

Chen, E.Y., Tan, C.M., Kou, Y., Duan, Q., Wang, Z., Meirelles, G.V., Clark, N.R., and Ma'ayan, A. (2013). Enrichr: interactive and collaborative HTML5 gene list enrichment analysis tool. BMC Bioinformatics *14*, 128.

Jolma, A., Yan, J., Whitington, T., Toivonen, J., Nitta, K.R., Rastas, P., Morgunova, E., Enge, M., Taipale, M., Wei, G., *et al.* (2013). DNA-binding specificities of human transcription factors. Cell *152*, 327-339.

Kuleshov, M.V., Jones, M.R., Rouillard, A.D., Fernandez, N.F., Duan, Q., Wang, Z., Koplev, S., Jenkins, S.L., Jagodnik, K.M., Lachmann, A., *et al.* (2016). Enrichr: a comprehensive gene set enrichment analysis web server 2016 update. Nucleic acids research *44*, W90-97.

Macisaac, K.D., Gordon, D.B., Nekludova, L., Odom, D.T., Schreiber, J., Gifford, D.K., Young, R.A., and Fraenkel, E. (2006). A hypothesis-based approach for identifying the binding specificity of regulatory proteins from chromatin immunoprecipitation data. Bioinformatics *22*, 423-429.

Maere, S., Heymans, K., and Kuiper, M. (2005). BiNGO: a Cytoscape plugin to assess overrepresentation of gene ontology categories in biological networks. Bioinformatics *21*, 3448-3449.

Mattis, V.B., Tom, C., Akimov, S., Saeedian, J., Ostergaard, M.E., Southwell, A.L., Doty, C.N., Ornelas, L., Sahabian, A., Lenaeus, L., *et al.* (2015). HD iPSC-derived neural progenitors accumulate in culture and are susceptible to BDNF withdrawal due to glutamate toxicity. Human molecular genetics *24*, 3257-3271.

Merico, D., Isserlin, R., Stueker, O., Emili, A., and Bader, G.D. (2010). Enrichment map: a network-based method for gene-set enrichment visualization and interpretation. PLoS One *5*, e13984.

Muller, F.J., Schuldt, B.M., Williams, R., Mason, D., Altun, G., Papapetrou, E.P., Danner, S., Goldmann, J.E., Herbst, A., Schmidt, N.O., *et al.* (2011). A bioinformatic assay for pluripotency in human cells. Nat Methods *8*, 315-317.

Okita, K., Matsumura, Y., Sato, Y., Okada, A., Morizane, A., Okamoto, S., Hong, H., Nakagawa, M., Tanabe, K., Tezuka, K., *et al.* (2011). A more efficient method to generate integration-free human iPS cells. Nat Methods *8*, 409-412.

Sareen, D., Ebert, A.D., Heins, B.M., McGivern, J.V., Ornelas, L., and Svendsen, C.N. (2012). Inhibition of apoptosis blocks human motor neuron cell death in a stem cell model of spinal muscular atrophy. PloS one *7*, e39113.

Shannon, P., Markiel, A., Ozier, O., Baliga, N.S., Wang, J.T., Ramage, D., Amin, N., Schwikowski, B., and Ideker, T. (2003). Cytoscape: a software environment for integrated models of biomolecular interaction networks. Genome Res *13*, 2498-2504.

Wingender, E., Dietze, P., Karas, H., and Knuppel, R. (1996). TRANSFAC: a database on transcription factors and their DNA binding sites. Nucleic acids research *24*, 238-241.